Environ. Sci. Technol. **1998**, *32,* 3980−3985

Mechanism of Pyrene Photochemical Oxidation in Aqueous and Surfactant Solutions

MICHAEL E. SIGMAN,*,†,‡
PETER F. SCHULER,‡
MRIGANKA M. GHOSH,‡ AND
R. T. DABESTANI†

Chemical and Analytical Science Division, Oak Ridge National Laboratory, P.O. Box 2008, MS 6100, Oak Ridge, Tennessee 37831-6100, and Department of Civil and Environmental Engineering and Center for Environmental Biotechnology, University of Tennessee, Knoxville, Tennessee 37996-2010

The photolysis of pyrene has been studied in water and in Brij 35 micellar media. Photolysis in both media lead to the formation of 1,6- and 1,8-pyrenequinones as stable products. The first step in the photochemical oxidation is proposed to involve an electron transfer from the excited singlet state of pyrene to molecular oxygen in a contact charge-transfer pair. The effects of oxygen and $HgCl_2$ on the photolysis are interpreted as ruling out mechanistic involvement of a triplet state of pyrene. 1-Hydroxypyrene is identified as a product of the initial photochemical oxidation. In the optically dilute aqueous solutions, 1-hydroxypyrene undergoes further photochemical oxidation to produce 1,6- and 1,8-pyrenequinones. Pyrene photolysis quantum yields are decreased by a factor of approximately 2 in the micellar media relative to the quantum yields determined in water. Fluorescence data suggest that pyrene resides in the micelles among the polyoxyethylene portion of the surfactant and not within the core of the micelle.

Introduction

Pyrene and other polynuclear aromatic hydrocarbons (PAH) are very persistent in the environment due to their resistance to biological degradation. This is especially true for PAH that consist of four or more rings. These multi-ring organic molecules are also very insoluble in water (i.e., pyrene has a water solubility of 0.135 mg/L) (*1*) and bind quite well to organic materials present in the subsurface. Therefore, once these larger PAH are released into the environment or subsurface, they are extremely difficult to remediate.

PAH are generated whenever organic materials (petroleum, coal, tobacco, or even hamburger) are combusted, burned, or cooked. PAH are also produced during energy-related chemical processing involving incomplete combustion, such as coal gasification and petroleum refining (*2*). Wastewaters and sludges generated in these processes contain PAH. Prior to the enactment of the Clean Water Act and the Resource Conservation and Recovery Act (RCRA), many of these wastewaters and sludges were directly discharged into receiving streams, where PAH accumulate in the sediment, or disposed of in unlined earthen lagoons. The non-biodegradable and hydrophobic characteristics of PAH have allowed many of these waste sites to remain intact to the present day.

Excavation and incineration of soil and/or sediment have been utilized at some sites; however, this has proven to be an expensive and socially unpopular remediation technique. Biological remediation would probably be a more acceptable process than incineration if the PAH could be made bioavailable in a cost-conscious manner. Previous studies have shown that soil washing with surfactant solutions can remove significant amounts of PAH from weathered soil collected from a manufactured gas plant site in upstate New York (*3, 4*). The studies demonstrated that Brij 35 [$C_{12}H_{25}(OCH_2CH_2)_{23}OH$, critical micelle concentration (cmc) = 9.2×10^{-5} M or 0.110 g L^{-1}] (*5*) solubilized more PAH than other surfactant solutions tested. In this study, Brij 35 has been utilized in all of the surfactant experiments.

Multiple studies have demonstrated that PAH undergo fairly rapid transformations in organic and aqueous solutions when exposed to ultraviolet light (*6*−*8*). A few studies provide identification of the photoproducts, provide determinations of relative biodegradability of the photoproducts and starting compounds, and/or have been conducted with PAH in surfactant solutions. Photolysis of benzo[*a*]pyrene in methanol followed by incubation in soil or sewage sludge demonstrated a noticeable increase in biodegradability and a decrease in mutagenicity (*9*). Thus, it would appear that, at least in some cases, more biodegradable products are formed from the photolysis of PAH.

The mechanism of photochemical degradation of pyrene and other PAH was addressed sometime ago, and evidence was presented to suggest that the mechanism involved a single electron oxidation process (*6*). A later study of anthracene photolysis in water determined that in the presence of oxygen the initial photoproducts were anthracene-9,10-endoperoxide, 9,10-anthraquinone, 10-hydroxyanthrone, and 9,10-dihydro-9,10-dihydroxyanthracene (*10*). The mechanism of endoperoxide formation was assigned to a geminate reaction of singlet molecular oxygen and anthracene within the solvent cage. The origin of the other products was less certain; however, an electron transfer mechanism was advanced. In oxygen-deficient aqueous solutions, the products from photolysis of anthracene were isomers of 9,9′,-10,10-tetrahydro-10,10′-dihydroxy-9,9′-bianthryl, which was proposed to result from an electron transfer mechanism. Mill and co-workers identified 7,12-benz[*a*]anthracenequinone (30%) as a photoproduct from the photolysis of aqueous solutions of benz[*a*]anthracene (*11*). Fatiadi has examined the photolysis of pyrene adsorbed on garden soil and an assortment of other solid supports (*12*). Photolysis on soil led to five identifiable photoproducts; 1,1′-bipyrene, 1,6- and 1,8-pyrenequinones, and 1,6- and 1,8-pyrenediols.

A study of the photolysis of PAH (pyrene, anthracene, naphthalene, and 7,12-dimethylbenzo[*a*]anthracene) in aqueous surfactant solutions was conducted to examine the effect of anionic surfactant concentration on the quantum yield of photolysis (*13*). The study demonstrated that above the cmc the quantum yields decreased significantly in sodium dodecyl sulfate (SDS) micellar media and increased slightly in sodium 1-decylbenzene sulfonate micelles. The study demonstrated that micellar media could affect the quantum yields of PAH photolysis, although greater photochemical and photophysical mechanistic details would enhance our understanding of the observed effect.

* To whom correspondence should be addressed. Phone: (423)576-2173; fax: (423)574-4902; e-mail:sigmanme@ornl.gov.
† Oak Ridge National Laboratory.
‡ University of Tennessee.

10.1021/es9804767 CCC: $15.00
Published on Web 11/10/1998

The first objective of the study presented in this paper was to determine the photoproducts and mechanism of pyrene photolysis in water and in aqueous Brij 35 surfactant solutions. In addition, it was our objective to explain any observed surfactant influence and to assess possible consequences for post-soilwashing photochemical treatment of PAH to enhance biodegradation.

Materials and Methods

Chemicals. Pyrene, ethyl acetate, chloroform-*d*, and nonionic surfactant Brij 35 were obtained from Aldrich Chemical Co. and used without further purification. Pyrene was determined to be 99.8% pure by a Hewlett-Packard 5890 series II gas chromatograph (GC). Sodium dichromate dihydride, cyclohexane, mercuric chloride, and HPLC-grade water were purchased from J. T. Baker and used without further purification. Methylene chloride, chloroform, and anhydrous sodium sulfate were obtained from EM Science and used without further purification. Glacial acetic acid was obtained from Mallinckrodt, Inc. and used without further purification. All solvents used in these experiments were HPLC grade. All other chemicals not specifically mentioned above were reagent grade and were used without additional purification.

Synthesis of Pyrenequinones. 1,6- and 1,8-pyrenequinones were synthesized based on literature procedures (*14*, *15*). Purification of the 1,6- and 1,8-pyrenequinones was accomplished by chromatography on a Chromatotron (model 7924T, Harrison Research) eluting with a 40% ethyl acetate in cyclohexane solution. A Hewlett-Packard model 1090 liquid chromatograph (LC) fitted with a reverse phase (C18) column and a diode array detector (LC−UV/VIS) confirmed the purity of the synthesized derivatives. Molecular structure and identification of derivatives were confirmed by comparison of NMR, LC−MS, and UV/VIS spectra with literature values (*14*−*16*). NMR spectra were measured with a Bruker 400 Hz spectrometer. LC−MS measurements were conducted with a Hewlett-Packard 1090 LC (fitted with a C18 column) connected to a Hewlett-Packard 5989B mass spectrometer through a thermal spray interface. UV/VIS spectra were determined with a Cary 4E UV/VIS spectrophotometer with 1 mm path length.

Upon isolation, 1,6-pyrenequinone was a yellow, slightly orange, solid that produced an orange-red color when dissolved in concentrated sulfuric acid. ^{1}H NMR (400.13 MHz, $CDCl_3$) δ 6.68 (d, 2H, $J = 9.79$ Hz), 7.65 (d, 2H, $J = 9.78$ Hz), 7.83 (d, 2H, $J = 7.28$ Hz), 8.47 (d, 2H, $J = 7.72$ Hz); ^{13}C NMR (100.63 MHz, $CDCl_3$) δ 127.2, 130.0, 130.2, 130.7, 133.7, 141.1, 185.4; high-resolution mass spectrum calculated for $C_{16}H_8O_2$ of 234.059, found 234.058. The observed UV/VIS spectra for 1,6-pyrenequinone agreed with previously reported data (*15*, *16*).

Upon isolation, 1,8-pyrenequinone was an orange-red solid that produced an olive-green color when dissolved in concentrated sulfuric acid. ^{1}H NMR (400.13 MHz, $CDCl_3$) δ 6.67 (d, 2H, $J = 9.86$ Hz), 7.67 (s, 2H), 7.68 (d, 2H, $J = 9.64$ Hz), 8.63 (s, 2H); ^{13}C NMR (100.63 MHz, $CDCl_3$) δ 127.6, 129.5, 129.6, 131.1, 131.2, 132.3, 141.5; high-resolution mass spectrum calculated for $C_{16}H_8O_2$ of 234.059, found 234.059. The observed UV/VIS spectra for 1,8-pyrenequinone agreed with previously reported data (*15*, *16*).

Solution Preparation. Aqueous pyrene and 1-hydroxypyrene solutions were prepared by placing small amounts (3−5 mg) of crystalline material in 1−2 L of distilled/deionized water (Millipore Milli-QUV Plus) in large Erlenmeyer flasks. The resulting mixtures were then wrapped in aluminum foil and stirred with a magnetic stirrer for at least 48 h. Aqueous pyrene solutions were then filtered through a medium porosity fritted glass funnel to remove any microcrystalline pyrene. Typical pyrene concentrations ranged from 0.08 to 0.11 mg L^{-1} as measured by UV/VIS absorbance at 334 nm. Typical 1-hydroxypyrene concentrations were similar to the pyrene concentrations as measured by UV/VIS absorbance at 386 nm.

Surfactant pyrene solutions were prepared using two different methods at concentrations of 0.1 g L^{-1} (sub cmc) and 4.0 g L^{-1} (above cmc) Brij 35. The first method (pyrene nonexcess conditions) used the procedure outlined above for preparing an aqueous pyrene solutions without the filtration step. After 48 h, 40-mL aliquots of the aqueous pyrene solution were transferred to 50-mL sample vials with screw cap lids. Sufficient Brij 35 was then added to achieve 0.1 and 4.0 g L^{-1} surfactant concentrations. After the vials were vigorously shaken to dissolve all of the Brij 35, the solutions were wrapped in aluminum foil and left to sit for at least 48 h to allow the surfactants to fully equilibrate. These solutions were then filtered through a fritted glass funnel, and the pyrene concentration was measured by a UV/VIS prior to use. The resulting solutions typically contained pyrene at concentrations similar to those observed in the absence of surfactant. These solutions were used for quantum yield determinations

The second method (pyrene excess condition) used to prepare surfactant solutions added a large excess of pyrene and required that the pyrene, Brij 35, and deionized water be simultaneously mixed together. Deionized water (50 mL) was added to approximately 2.0 mg of pyrene and either 5 mg (0.1 g/L) or 200 mg (4.0 g/L) of Brij 35. The resulting mixture was then placed in a stoppered Erlenmeyer flask, wrapped in aluminum foil, and stirred with a magnetic stirrer for at least 48 h. Prior to use in experiments, these surfactant solutions were filtered through a fritted glass funnel, and the pyrene concentration was measured by a UV/VIS. All solutions were prepared without degassing or manipulating the pH, unless specifically stated elsewhere.

Determination of Pyrene and 1-Hydroxypyrene Photolysis Rates and Quantum Yields. The initial pyrene and 1-hydroxypyrene concentrations were determined by UV/VIS. Then approximately 3 mL of the aqueous or surfactant solution containing the aromatic hydrocarbon was transferred to a quartz cell containing a magnetic stir bar. The quartz cell had a 1-cm path length and a Teflon-lined screw cap. Solutions were then irradiated in a Rayonet RPR-100 photoreactor (Southern New England Ultraviolet) equipped with 350-nm bulbs while stirred by a magnetic stirrer. The lamps were allowed to warm for at least 30 min prior to sample photolysis. Photon flux was measured with an IL 700 photoradiometer, 1 nm band-pass (International Light Inc.). The lamp flux was measured at 10-nm increments in the 300−400 nm range. Maximum output from the lamps was 5.18×10^{14} photons cm^{-2} s^{-1} (at 350 nm) with a numerically integrated output of 2.20×10^{16} photons cm^{-2} sec^{-1} between 300 and 400 nm. Residual pyrene and 1-hydroxypyrene were determined at various photolysis times by measuring the fluorescence with a Fluorolog 1680 double spectrofluorometer (Spex Industries, Inc.).

Emission scans of the pyrene and 1-hydroxypyrene fluorescence in optically dilute solutions were measured from 275 to 600 nm and from 350 to 600 nm, respectively. Pyrene and 1-hydroxypyrene were excited at 240 and 285 nm, respectively. Measurements of fluorescence intensity (F) were recorded at the emission peaks that occurred at approximately 372 and 392 nm for pyrene and at 386 for 1-hydroxypyrene. Disappearance rates of both pyrene and 1-hydroxypyrene from optically dilute solutions were determined to follow apparent first-order kinetics by plotting ln (F^o/F) versus time, and the slope of the linear plot was used to determine the photolysis rate and half-life. The rate data were used to calculate the quantum yields for pyrene and 1-hydroxypyrene consumption as previously reported (*17*−*20*).

The effect of oxygen on the photolysis rate in optically dilute solutions was determined as follows. A solution of pyrene in water (without surfactant) was purged with Ar (30 min purge) in a 1-cm quartz cell sealed with a rubber septum and photolyzed as described above.

Solutions prepared under "pyrene excess conditions" with 4 g L^{-1} Brij 35 were not optically dilute, and the disappearance of pyrene followed apparent zero-order kinetics. In these solutions, pyrene loss was followed directly by monitoring the absorption spectrum of pyrene in a 0.1-cm path length cell.

Photolysis of Pyrene and 1-Hydroxypyrene for Product Identification in Aqueous Solutions. After measuring the initial pyrene concentration by UV/VIS, 80-mL aliquots of the solutions were placed in quartz tubes (2.5 cm in diameter and 29 cm long) with Teflon screw caps. Several batches of solutions were then irradiated. Due to the extremely low solubility of pyrene and 1-hydroxypyrene in water, a total of between 1 and 1.5 L of solution was irradiated and processed according to the following procedure. After photolysis, the organic components were removed from solution by vacuum filtration through a 1 mL/100 mg Accubond SPE cartridge (J&W Scientific). The organic compounds were then washed from the SPE cartridge with 5−10 mL of acetonitrile into a small Erlenmeyer flask. Anhydrous sodium sulfate (EM Science) was then added to the acetonitrile to remove any residual water. After decanting the acetonitrile solution into a small round-bottom flask and rinsing the sodium sulfate with additional acetonitrile, the resulting solution was evaporated to dryness with a rotory evaporator. One milliliter of acetonitrile was then used to dissolve the dried organic residual. This solution was then pipetted into an amber crimp vial and wrapped in aluminum foil to await analysis.

Identification/Quantification of Photolysis Products. Products of pyrene photolysis were identified by LC−UV/VIS (Hewlett-Packard 1090) by matching retention times and UV/VIS spectra with synthesized derivatives and by LC−MS. The LC was operated with a 65/35 water to acetonitrile ratio at a liquid flow rate of 0.21 mL/min. Quantification of the pyrene and pyrenequinones was conducted after calibration of the LC−UV/VIS with known concentrations of solutions containing pyrene or synthesized pyrenequinones. Photochemical products from 1-hydroxypyrene were identified by LC−UV/VIS by matching the retention times and spectra with authentic materials.

Determination of Reactivity with Singlet Oxygen. A 0.5 M solution of pyrene was prepared in a 9:1 mixture of methylene chloride and methanol. A small amount of methylene blue was then added to this solution to photochemically sensitize the formation of singlet molecular oxygen. Photolysis of this solution, under air, was conducted in a Rayonet RPR-100 photoreactor equipped with a merry-go-round and 650-nm bulbs. Samples of the solutions were analyzed by UV/VIS and GC to determine the extent of pyrene degradation.

Oxygen Quenching of Pyrene Fluorescence in Water. A solution of pyrene in water (without surfactant) was prepared and filtered as previously described. The sample was placed in a 1-cm quartz cell and sealed with a rubber septum. The sample was purged with Ar for 20 min to remove dissolved oxygen. The pyrene fluorescence spectrum was measured immediately after purging with Ar. The septum was removed from the cell, and the sample was allowed to equilibrate with air in the dark. The fluorescence spectrum was recorded after 180 and 240 min equilibration times. The two fluorescence spectra taken after opening the cell to air were of approximately the same intensity, and both had less intense pyrene fluorescence than the Ar-purged sample.

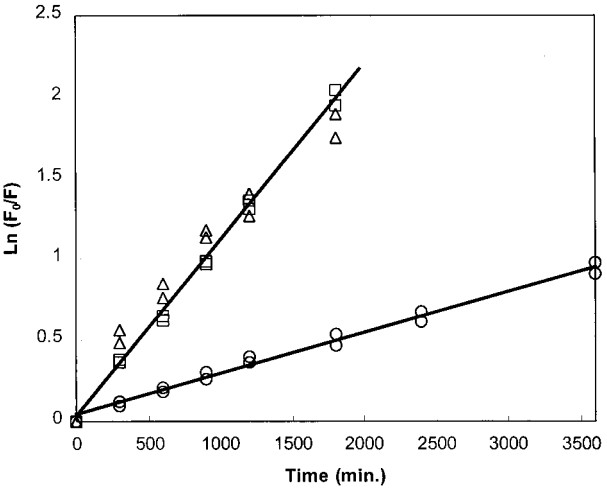

FIGURE 1. Apparent first-order kinetic plot of the photochemical degradation of pyrene in air-saturated water (triangle), water containing 1.2 × 10^{-3} M $HgCl_2$ (square), and argon-purged water (circle).

Results and Discussion

Photolysis of Pyrene and 1-Hydroxypyrene in Aqueous Solutions. Pyrene underwent apparent first-order photolytic decomposition in aereated and argon-purged aqueous solutions and in aqueous solutions containtaining 1.2 × 10^{-3} M $HgCl_2$ (Figure 1). The rate of photochemical decomposition was not affected by the addition of $HgCl_2$; however, removal of oxygen by argon purge slowed the photochemical decomposition by approximately a factor of 4. The quantum yields for the photodecomposition were calculated from the apparent first-order decomposition rates as previously described for optically dilute solutions (*17*−*20*). The quantum yields in aerated water, with or without $HgCl_2$, was 2.11 (± 0.14) × 10^{-3}, whereas the quantum yield in argon-purged water was 5.19 (± 0.13) × 10^{-4}. The quantum yield for photodegradation in air-saturated water agrees quite well with previously published values of 2.2 (± 0.3) × 10^{-3} (at 366 nm) and 2.0 (± 0.3) × 10^{-3} (at 313 nm) (*6*). These results show that oxygen plays an important role in the mechanism of pyrene photochemical degradation in water; however, a triplet state of pyrene is probably not involved in the oxidation mechanism. If a triplet state of pyrene was involved, the quantum yield of photolysis would be greatly decreased by $HgCl_2$, a known triplet quencher (*21*). Zepp reported that the kinetics of 9-methylanthracene photodegradation in water was similarly unaffected by the presence of $HgCl_2$ (*6*). However, Zepp also reported that the removal of oxygen had no effect on the photolysis of 9-methylanthracene (*6*), whereas removal of oxygen is observed to significantly slow the photochemical degradation of pyrene in water. In agreement with our observations, Mill reported that nitrogen-purging aqueous samples of benzo[*a*]pyrene and benz[*a*]-anthracene greatly inhibited their photochemical degradation (*11*).

Photolysis of pyrene in water led to the formation of 1,6- and 1,8-pyrenequinones, which have the chemical structures as shown in Scheme 1. Material balances of pyrene and 1,6- and 1,8-pyrenequinones for photolysis times between 7.5−30 min (0.75 to 3.0 half-lives) are presented in Table 1. The quinones and unreacted pyrene accounted for 74−91% of the starting material. Additional photoproducts (including the corresponding 1,6- and 1,8-dihydroxypyrenes and 1-hydroxypyrene) are present in trace amounts. The observed ratio of 1,6-pyrenequinone to 1,8-pyrenequinone varied from 1.09 to 1.96, largely due to incomplete chromatographic separation of the isomeric products and associated integra-

SCHEME 1

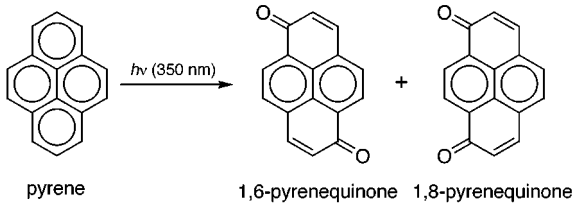

tion error. A quinone ratio of 1.10 was determined for the most concentrated sample examined, after photolysis for 90 min. Significant quantities of other photoproducts were not present in the sample, as determined by LC, and the integration appeared to be more accurate than that determined in more dilute solutions.

The quantum yield for 1-hydroxypyrene photolysis in aerated water was determined to be $2.77\ (\pm 0.25) \times 10^{-3}$. The products from photolysis were determined to be 1,6- and 1,8-pyrenequinones. No other products were formed in significant quantities. The yields of the pyrenequinones were not quantitated.

Effect of a Nonionic Surfactant on the Photolysis of Pyrene. When pyrene−surfactant solutions were prepared under the pyrene nonexcess conditions (vide supra), the photolysis efficiency was only slightly reduced, relative to photolysis in water alone. The quantum yield for consumption of pyrene in the optically dilute solutions decreased to $1.26\ (\pm 0.07) \times 10^{-3}$. Solutions prepared under pyrene excess conditons with 0.1 g L^{-1} Brij 35 were also optically dilute; however, fluorescence spectra from the solutions revealed both monomer and excimer emissions. Excitation spectra monitored under the excimer emission were red-shifted by approximately 3 nm relative to spectra recorded by monitoring the monomer emission. The spectral shift exceeds the spectrometer bandwidth (1.46 nm), suggesting that the excimer emission is not dynamic in origin. Upon photolysis, the source of excimer emission was consumed faster than monomer. The quantum yield for pyrene consumption, after the depletion of all excimer emission, was $9.4\ (\pm 0.7) \times 10^{-4}$.

The pyrene concentration in solutions prepared under pyrene excess conditions with 4 g L^{-1} Brij 35 were much higher (approaching 30 mg L^{-1}). These solutions were no longer optically dilute, and pyrene consumption became an apparent zero-order process. Excimer fluorescence was also observed in these solutions; however, the excitation spectra monitored under both the monomer and excimer emissions were identical. The result indicates that the excimers formed in this solution are dynamic (i.e., they form during the excited state lifetime of pyrene and do not result from ground-state complexes). The presence of a small amount of static excimer in the solutions could not be ruled out. The quantum yield for pyrene photodegradation was determined to be $1.0\ (\pm 0.1) \times 10^{-3}$. This value is not significantly different from the quantum yields reported here for pyrene consumption in the other Brij 35 solutions.

In Figure 2, curve A, shows the fluorescence spectrum of pyrene in water without surfactant. The spectrum shows the well-known vibrational structure of pyrene, and there is no evidence for excimer emission. The absence of excimer is significant because it testifies to the fact that there are no ground-state pairs or microcrystals of pyrene detectable by this highly sensitive technique. Curve B in the figure shows the fluorescence of pyrene in the presence of Brij 35 (4.0 g L^{-1}) in a solution prepared under pyrene nonexcess conditions. The spectrum shows that the ratio of the first and third vibronic bands in the monomer have changed significantly and that a very small amount of pyrene excimer (centered at 480 nm) is present. The change in the vibronic intensities is a well-studied phenomena in pyrene and reflects the fact that the pyrene exists primarily inside the micelles (vide infra). The small amount of excimer present likely results from the increased localized concentration within the micelles. Curve C shows the fluorescence of pyrene in a solution containing Brij 35 (4.0 g L^{-1}) that was prepared by under the pyrene excess conditions (vide supra). The relative intensities of the first and third vibronic bands in the monomer emission are essentially the same as in curve B; however, a large excimer emission is now observed. The excimer emission results from the pyrene solubility enhancement due to the presence of the surfactant.

The nature of the pyrene monomer's chemical environment in solution can be determined from the fine structure of the fluorescence spectra shown in Figure 2. The intensity of the first vibronic band (372 nm, I_1) relative to that of the third band (384 nm, I_3) provides an empirical measure of the polarity of the pyrene surrounding environment and forms the basis for the P_y solvent polarity parameter (*22*). The value of P_y for hexane has been reported to be 0.58, whereas the values for ethyl ether, ethanol, and triethylene glycol are reported to be 1.02, 1.18, and 1.57, respectively (*22*). The observed P_y value determined for water in our laboratory (Figure 2, curve A) was 1.84 ± 0.04, which agrees with published values of 1.87 (22). As the concentration of Brij 35 was increased, the P_y value was reduced as shown in Table 2. The P_y values of 1.22−1.28 measured at 4 g L^{-1} Brij 35 are in fairly good agreement with a previously reported value of 1.18 (*23*). The size of the P_y value in the presence of high concentrations of Brij 35 suggests that the pyrene resides among the polyoxyethylene groups of the surfactant. If the pyrene molecules resided within the hydrophobic core of the micelle, we would expect the measured P_y values to be similar to those of hydrocarbon solvents, such as hexane. The sizable red-shift of the excimer fluorescence relative to the monomer emission ($-\Delta H_{excimer} \sim 9$ kcal mol^{-1}) allows for determination of the ratio I_1/I_3 for all solutions.

Proposed Mechanism of Pyrene Photolysis. Two possible mechanisms have been proposed for the oxidative photolysis of pyrene in water: (i) electron transfer and (ii) singlet molecular oxygen addition (*6*, *7*). Singlet molecular oxygen was not observed to react with pyrene in our laboratory. In addition, the regiochemistry of pyrene oxidation in water is not indicative of known singlet molecular oxygen reactions. Singlet molecular oxygen addition to aromatic systems can occur at adjacent carbons to give a dioxetane, at carbons bearing a 1,4 relationship to give an endoperoxide or at other conjugated carbons, provided addition can occur in a pericyclic fashion. On the basis of these observations, we favor an electron transfer mechanism.

One electron oxidation of pyrene by excited state electron ejection is a possible mechanism of forming the radical cation. Photoionization of naphthalene in acetonitrile has been reported to be a monophotonic process (*24*); however, the process in aqueous acetonitrile was later reported to be biphotonic (*25*). The photon flux in our photoreactors is too low to promote a biphotonic process. An alternative, monophotonic, mechanism for electron transfer oxidation is through excitation of pyrene−oxygen contact charge transfer pairs, as depicted in step 1 of Scheme 2. Contact charge transfer pairs of aromatic hydrocarbons and oxygen are well-known in polar organic solutions and have also been reported in micellar media (*26*). A pyrene−oxygen contact charge transfer pair has been reported in chloroform at high oxygen-pressures (*27*). The absorption spectra of pyrene in oxygen purged (curve A) and nitrogen-purged (curve B) water at atmospheric pressure are shown in Figure 3. The absorption has been normalized at 335 nm to correct for pyrene loss upon purging with nitrogen or oxygen. The spectral change in the presence of oxygen shows a weakly

TABLE 1. Mole Percent Remaining Pyrene and Quinone Products Formed at Various Times during Pyrene Photolysis in Aerated Water

photolysis time (min)	pyrene remaining	1,6-pyrenequinone	1,8-pyrenequinone	ratio of 1,6- to 1,8-quinones	material balance[a] (%)
7.5	59.0	15.6	14.3	1.09	88.9
15	43.0	31.8	16.2	1.96	91.0
30	16.4	33.8	23.3	1.45	73.5

[a] Material balance = $(A_t + A_{prod})/A_o \times 100\%$, where A_{prod}, A_o, and A_t are the amount of product (1,6- and 1,8-pyrenequinones), pyrene at time zero, and pyrene at time t, respectively.

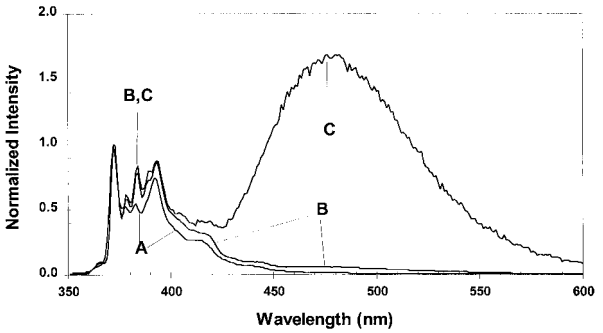

FIGURE 2. Fluorescence spectra of (A) pyrene in water without surfactant, (B) pyrene (nonexcess) with Brij 35 (4 g L^{-1}) in water, and (C) pyrene (excess) with Brij 35 (4 g L^{-1}) in water. Spectra were normalized at 372 nm. See text for description of nonexcess and excess conditions.

TABLE 2. Effect of Surfactant Concentration and Method of Solution Preparation on Measured P_y Values

solution description	preparation method	$P_y \pm$ SD
aqueous, no Brij 35		1.84 ± 0.04
0.1 g/L Brij 35	nonexcess pyrene	1.49 ± 0.02
	excess pyrene	1.59 ± 0.03
4.0 g/L Brij 35	nonexcess pyrene	1.28 ± 0.01
	excess pyrene	1.22 ± 0.06

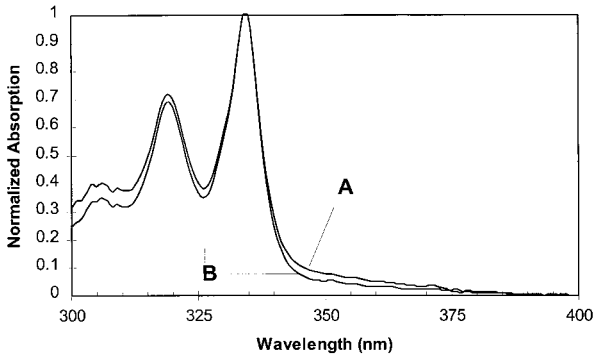

FIGURE 3. Absorption spectra of pyrene in oxygen-purged (A) and nitrogen-purged (B) water at atmospheric pressure. The absorption spectra have been normalized at 335 nm to correct for pyrene loss upon purging.

increased absorption on the red edge of the lowest energy electronic transition. Additional intensity can also be seen on the blue edge of the first envelope of states, similar to that observed for benzene in the vapor phase (*28*).

Several research groups have studied solvent effects on 1-methylnaphthalene−oxygen contact charge transfer pairs in oxygenated solutions under atmospheric pressure (*29, 30*). It has been shown that in a nonpolar solvent (cyclohexane), the primary decay route for the excited complex gave the localized triplet state of 1-methylnaphthalene. In a polar solvent (acetonitrile), the quantum yield for formation of the

SCHEME 2

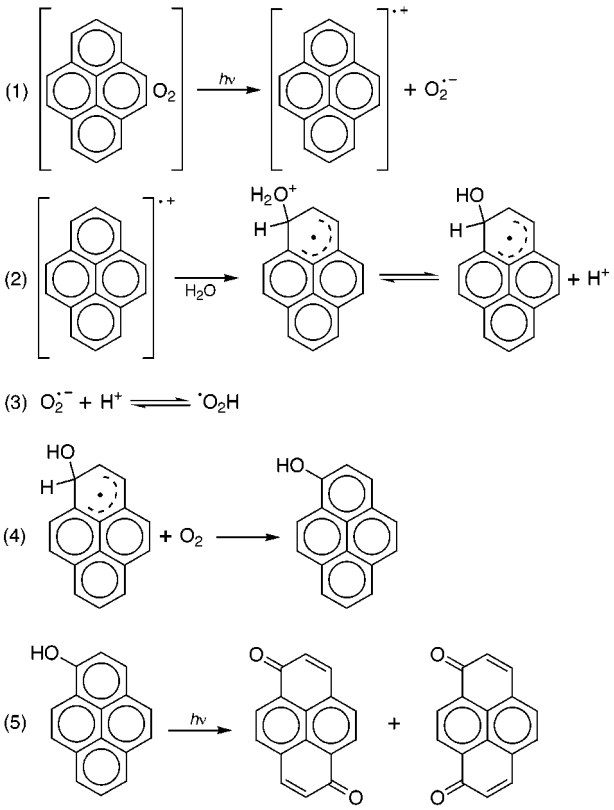

localized triplet state decreased by 50% and an additional pathway for excited state decay became available. The new pathway in polar solvent was attributed to decay of the excited state to regenerate the ground state pair. Photoproduct studies were not included with the transient studies of 1-methylnaphthalene−oxygen contact charge transfer pairs. In highly polar media, such as water, the charge transfer state would be further stabilized, possibly to give solvent separated ionic species, and additional chemistries could arise from a pyrene radical cation and superoxide.

Trapping of the pyrene radical cation by water with subsequent deprotonation would give a hydroxypyrenyl radical along with a proton as shown in step 2 of Scheme 2. Water has previously been proposed to trap radical cations formed during photolysis and radiolysis of pyrene on inorganic oxide supports (*31, 32*). Water trapping of the radical cation of naphthalene has been observed to occur at a rate of 4.0×10^4 M^{-1} s^{-1} (*25*). Step 3 of Scheme 2 depicts the acid−base equilibrium involving the hydroperoxyl radical. The pK_a of the hydroperoxyl radical is reported to be 4.4−4.8, and the radical will be highly dissociated in water at a pH of 7−8 (*33, 34*). The hydroxypyrenyl radical can be readily oxidized in solution to give 1-hydroxypyrene, as shown in step 4 of Scheme 2. The radical cation of pyrene, formed by ionizing radiation on silica−alumina, has been shown to react with water to form 1-hydroxypyrene (*32*). The presence of

molecular oxygen was reported to increase the yield of 1-hydroxypyrene, as was the oxidant $Fe(CN)_6^{3-}$. The oxidant involved in step 4 of Scheme 2 is probably molecular oxygen in our system. The oxidation of the radical may be fairly facile in aerated water, where the concentration of oxygen is $\sim 2.5 \times 10^{-4}$ M. The rate of hydrogen atom abstraction by radicals to generate olefins has been reported to be as high as 1×10^8 M^{-1} s^{-1} in the liquid phase (*35*). The rate for hydrogen atom abstraction from the radical shown in Scheme 2 may be expected to be at least this fast and possibly faster given the aromaticity of the final product. The pseudo-first-order rate for oxidation of the intermediate radical would be expected to be a minimum of 2.5×10^4 s^{-1} ($\tau = 4$ μs), which is very fast relative to the rate of pyrene consumption in our system.

In a second photochemical event, shown in step 5 of Scheme 2, 1-hydroxypyrene is oxidized to give the quinones. This conversion could feasibly occur by a similar mechanism. Phenol and other oxygenated aromatics are known to undergo monophotonic electron ejection, upon electronic excitation, to generate the aryloxy radical and a proton (*36*). The aryloxy radical produced in this case would have multiple resonance structures, only two of which lead to the observed products. The exact mechanism of this conversion and the possible intermediate formation of 1,6- and 1,8-dihydroxypyrene are subjects for continued investigation in our laboratory.

The intermediate formation of 1-hydroxypyrene is supported by the observation that its photolysis leads to the same photoproducts formed from pyrene photolysis. Additionally, the quantum yield for photolysis of 1-hydroxypyrene is slightly larger than the quantum yield for photolysis of pyrene. Under the experimental conditions of optically dilute solutions employed in these experiments, the 1-hydroxypyrene would undergo facile photochemical conversion to products and little, if any, of this intermediate would be detectable in pyrene photolysis solutions.Perylene radcial cations are known to undergo a complex series of reactions to produce 3,10-perylenequinone (*37*). The series of reactions involves trapping the perylene radical cation with water, analogous to step 2 in Scheme 2, with subsequent oxidation steps requiring additional radical cations. The overall reaction has a stoichiometry requiring six radical cation species and two water molecules to produce one quinone. This same process is considered unlikely in the photochemical oxidation of pyrene in water. The limited aqueous solubility of pyrene and the absence of any pyrene association in water, as evidenced by the absence of pyrene excimer emission, make the bimolecular reactions unfavorable. However, the limited solubility of pyrene in water allows for multiple photochemical steps to occur, as detailed in Scheme 2. Additional support for the single electron transfer nature of the proposed oxidation comes from the reported bench-scale preparation of pyrenequinones from a Ce(IV)/Ce(III)-mediated electrochemical oxidation of pyrene (*38*).

The slight decrease in the photolysis quantum yield for pyrene in Brij 35 micellar media may result from a decreased ability of the medium to support charge separation. Pyrene appears to reside in the polyoxyethylene region of the surfactant micelles, which is less polar than water, as determined by the P_y parameter. The small decrease in the quantum yield would be minimally detrimental to post-soilwashing photochemical treatment of PAH to enhance biodegradation.

Acknowledgments

This research was supported by a fellowship from the University of Tennessee's Waste Management Research and Education Institute and by the Division of Chemical Sciences, Office of Basic Energy Sciences, U.S. Department of Energy under Contract DE-AC05-96OR22464 with Oak Ridge National Laboratory, managed by Lockheed Martin Energy Research Corp.

Literature Cited

(1) Mackay, D. *Multimedia Environmental Models: The Fugacity Approach*; Lewis Publishers: Chelsea, MI, 1991; p 45.
(2) Cerniglia, C. E. *Petroleum Microbiology*; Atlas, R. M., Ed.; Macmillan Publishers: New York, 1984; pp 99−128.
(3) Yeom, I. T.; Ghosh, M. M.; Cox, C. D.; Robinson, K. G. *Environ. Sci. Technol.* **1995**, *29*, 3015−3021.
(4) Yeom, I. T.; Ghosh, M. M.; Cox, C. D. *Environ. Sci. Technol.* **1996**, *30*, 1589−1595.
(5) Rosen, M. J. *Surfactants and Interfacial Phenomena*, 2nd ed.; John Wiley: New York, 1989; p 328.
(6) Zepp, R. G.; Schlotzhauer, P. F. *Polynuclear Aromatic Hydrocarbons*; Jones, P. W., Leber, P., Eds.; Ann Arbor Science Publishers: Ann Arbor, MI, 1979; pp 141−158.
(7) Shevchuk, I. *Eesti NSV Tead. Akad. Toim. Keemia*, **1986**, *35*, 128−133.
(8) Low, G. K.; Batley, G. E.; Brockbank, C. I. *J. Chromatogr.* **1987**, *392*, 199−210.
(9) Miller, R. M.; Singer, G. M.; Rosen, J. D.; Bartha, R. *Appl. Environ. Microbiol.* **1988**, *54*, 1724−1730.
(10) Sigman, M. E.; Zingg, S. P. In *Aquatic and Surface Photochemistry*; Helz, G. R., Zepp, R. G., Crosby, D. G., Eds.; CRC Press: Boca Raton, FL, 1994; pp 197−206.
(11) Mill, T.; Mabey, W. R.; Lan, B. Y.; Baraze, A. *Chemosphere* **1981**, *10*, 1281.
(12) Fatiadi, A. J. *Environ. Sci. Technol.* **1967**, *1*, 570.
(13) Checkulaev, V. P. *Eesti NSV Tead. Akad. Toim., Keem.* **1982**, *31*, 124−130.
(14) Cho, H.; Harvey, R. G. *J. Chem. Soc., Perkins Trans. I* **1976**, 836−839.
(15) Fatiadi, A. J. *J. Chromoatogr.* **1965**, *20*, 319−324.
(16) Pierce, R. C.; Katz, M. *Environ. Sci. Technol.* **1976**, *10*, 45−51.
(17) Hwang, H.; Hodson, R. E.; Lee, R. F. *Photochemistry of Environmental Aquatic Systems*; Zika, R. G., Cooper, W. J., Eds.; American Chemical Society: Washington, DC, 1987; pp 27−43.
(18) Lyman, W. J.; Reehl, W. F.; Rosenblatt, D. H. *Handbook of Chemical Property Estimation Methods*; McGraw-Hill: New York, 1982; pp 8-1−8-43.
(19) Leifer, A. *The Kinetics of Environmental Aquatic Photochemistry*; American Chemical Society: Washington, DC, 1988; pp 77−95.
(20) Shi, Z.; Sigman, M. E.; Ghosh, M. M.; Dabestani, R. T. *Environ. Sci. Tehcnol.* **1997**, *31*, 3581.
(21) Nilsson, R.; Merkel, P. B.; Kearns, D. R. *Photochem. Photobiol.* **1972**, *16*, 109−116.
(22) Dong, D. C.; Winnik, M. A. *Can. J. Chem.* **1984**, *62*, 2560−2565.
(23) Kalyanasundaram, K.; Thomas, J. K. *J. Am. Chem. Soc.* **1977**, *99*, 2039.
(24) Delcourt, M. O.; Rossi, M. J. *J. Phys. Chem.* **1982**, *86*, 3233.
(25) Steenken, S.; Warren, C. J.; Gilbert, B. C. *J. Chem. Soc., Perkins Trans. 2* **1990**, 335.
(26) Guardia, L. D.; King, A. D., Jr. *J. Colloid Interface Sci.* **1982**, *88*, 8.
(27) Slifkin, M. A.; Allison, A. C. *Nature* **1967**, *215*, 949.
(28) Birks, J. B.; Pantos, E.; Hamilton, T. D. S. *Chem. Phys. Lett.* **1973**, *20*, 544.
(29) Kuriyama, Y.; Ogilby, P. R.; Mikkelson, K. V. *J. Phys. Chem.* **1994**, *98*, 11918.
(30) Logunov, S. L.; Rodgers, M. A. J. *J. Phys. Chem.* **1993**, *97*, 5643.
(31) Mao, Y.; Thomas, J. K. *Langmuir* **1992**, 8, 2501.
(32) Mao, Y.; Iu, K. K.; Thomas, J. K. *Langmuir* **1994**, *10*, 709.
(33) Czapski, G.; Bielski, J. H. J. *J. Phys. Chem.* **1963**, *67*, 2180.
(34) Rabani, J.; Nielson, S. O. *J. Phys. Chem.* **1969**, *73*, 3736.
(35) Mill, T.; and Hendry, D. G. In *Comprehensive Chemical Kinetics*; Bamford, C. H., Tipper, C. F. H., Eds.; Elsevier: Amsterdam, 1980; p 28.
(36) Grossweiner, L. I.; Joschek, H.-I. *Adv. Chem. Ser.* **1965**, *50*, 279.
(37) Ristagno, C. V.; Shine, H. J. *J. Org. Chem.* **1971**, *36*, 4050.
(38) Wakamatsu, M.; Tsuji, A.; Olubo, I.; Yoshiyama, A.; Sato, N.; Nonaka, T. *Denki Kagaku* **1992**, *60*, 1005.

Received for review May 11, 1998. Revised manuscript received September 23, 1998. Accepted October 1, 1998.

ES9804767